



HAL
open science

Predictive score for complete occlusion of intracranial aneurysms treated by flow-diverter stents using machine learning

Alexis Guédon, Cédric Thépenier, Eimad Shotar, Joseph Gabrieli, Bertrand Mathon, Kévin Premat, Stéphanie Lenck, Vincent Degos, Nader Sourour, Frédéric Clarençon

► To cite this version:

Alexis Guédon, Cédric Thépenier, Eimad Shotar, Joseph Gabrieli, Bertrand Mathon, et al.. Predictive score for complete occlusion of intracranial aneurysms treated by flow-diverter stents using machine learning. *Journal of Neurointerventional Surgery*, 2021, 13 (4), pp.341-346. 10.1136/neurintsurg-2020-016748 . hal-03196093

HAL Id: hal-03196093

<https://hal.sorbonne-universite.fr/hal-03196093v1>

Submitted on 12 Apr 2021

HAL is a multi-disciplinary open access archive for the deposit and dissemination of scientific research documents, whether they are published or not. The documents may come from teaching and research institutions in France or abroad, or from public or private research centers.

L'archive ouverte pluridisciplinaire **HAL**, est destinée au dépôt et à la diffusion de documents scientifiques de niveau recherche, publiés ou non, émanant des établissements d'enseignement et de recherche français ou étrangers, des laboratoires publics ou privés.

1 Predictive Score for Complete Occlusion of Intracranial Aneurysms Treated by Flow-
2 Diverter Stents using Machine Learning

3
4
5 Original Research

6
7 Alexis Guédon, MD ^{*,8,9}, Cédric Thepenier, MD PhD ^{3,4}, Eimad Shotar, MD ², Joseph Gabrieli,
8 MD ⁵, Bertrand Mathon, MD ^{1,6}, Kévin Premat, MD ^{1,2}, Stéphanie Lenck, MD ², Vincent Degos,
9 MD PhD ^{1,7}, Nader Sourour, MD ², Frédéric Clarençon, MD PhD ^{1,2}

10
11
12
13 ¹ Sorbonne University, Paris, France

14 ² Department of Neuroradiology, Pitié-Salpêtrière Hospital, Paris, France

15 ³ Department of Experimental Neuropathology, Institut Pasteur, Paris, France

16 ⁴ French Armed Forces Biomedical Research Institute (IRBA), Brétigny-sur-Orge, France

17 ⁵ Department of Neuroradiology, University Hospital of Padova, Padova, Italy

18 ⁶ Department of Neurosurgery, Pitié-Salpêtrière Hospital, Paris, France

19 ⁷ Department of Neuro-anesthesiology, Pitié-Salpêtrière Hospital, Paris, France

20 ⁸ Department of Anatomy, University of Paris, Paris, France

21 ⁹ Biosurgical Research Lab (Carpentier Foundation), European Georges-Pompidou Hospital,
22 INSERM UMR_S 1140, University of Paris, Paris, France

23
24
25
26 ** Corresponding author and corresponding author for social networks:*

27 Pr Frédéric Clarençon, MD, PhD

28 Department of Neuroradiology,

29 Pitié-Salpêtrière Hospital,

30 Paris, France

31 Email: frederic.clarencon@aphp.fr

32 Tel: +33 1 84 82 73 00

33
34
35
36 **Cover Title:** Flow Diverter Stents: Prediction of Success

37
38
39
40 **Keywords:** Flow-diverter stent, Intracranial aneurysm, Machine learning, Occlusion status,
41 Predictive score

42
43
44
45
46
47 Word Count: 3118

48 Structured abstract: 248

49 Tables: 3, Illustrations: 1

50 References: 35

51
52
53
54
55

56 **Abstract**

57 *Background:* Complete occlusion of an intracranial aneurysm (IA) after the deployment of a
58 flow-diverter stent (FDS) is currently unpredictable. The aim of the study was to develop a
59 predictive occlusion score based on pre-treatment clinical and angiographic criteria.

60 *Methods:* Consecutive patients with ≥ 6 months follow-up were included from 2008 to 2019
61 and retrospectively analyzed. Each IA was evaluated by using the Raymond-Roy occlusion
62 classification (RROC) and dichotomized as occluded (A) or residual (B/C), and 80% of patients
63 randomly attributed to the training sample. Feature selection and binary outcome prediction
64 relied on logistic regression, and threshold maximizing class separation selected by a CART
65 tree algorithm. The feature selection was addressed by a genetic algorithm selecting among the
66 30 pre-treatment available variables.

67 *Results:* The study included 146 patients with 154 IAs. Feature selection yielded a combination
68 of six variables with a good cross-validated accuracy on the test sample, a combination we
69 labeled DIANES score (IA's diameter, indication, parent artery diameters ratio, neck ratio, side-
70 branch artery, and sex). A score > -6 maximized the ability to predict a RROC=A with
71 sensitivity of 87% (95%CI: 79%, 95%) and specificity of 82% (95%CI: 64%, 96%) on the training
72 sample. Accuracy was 86% (95%CI: 79%, 94%). In the test sample, sensitivity and specificity
73 were 89% (95%CI: 77%, 98%) and 60% (95%CI: 33%, 86%), respectively. Accuracy was 81%
74 (95%CI: 69%, 91%).

75 *Conclusion:* A score was developed as a grading scale for prediction of the final occlusion
76 status of IA treated with FDS.

77

78

79

80

81

82

83

84 **Introduction**

85 Flow-diverter stents (FDSs) have been widely accepted for the treatment of complex
86 intracranial aneurysms (IAs) (giant/large, large-necked, and/or dissecting/fusiform IAs) and in
87 case of IA recanalization [1]. The effect of FDS is based on two complementary mechanisms
88 that will eventually lead to IA thrombosis: diversion of the blood flow from the IA sac toward
89 the parent artery and endothelialization of the IA's neck promoting a neck sealing. The goal of
90 the treatment is the same as in coils embolization, i.e. a complete obliteration of the IA's sac,
91 assessed by the widely use three-point scale Raymond-Roy occlusion classification (RROC)
92 [2].

93 However, whether complete IA occlusion will occur after FDS deployment is currently
94 unpredictable. Indeed, the process of IA's sac thrombosis is progressive, with time course
95 ranging from several minutes to several months. In a significant number of cases, there is no
96 occlusion (as high as 24% at 6 months and 15% after one year) [1–3]. This delay generates
97 uncertainties for the patient and the operator, absence of early optimal protection against
98 (re)rupture and loss of intra-aneurysmal access because of the FDS's tight mesh. Pre-treatment
99 predisposing factors of complete IA occlusion would be very helpful in many clinical situations
100 to predict the most likely upcoming flow-diverting effect.

101 Several studies have already shown the existence of factors predictive of aneurysmal
102 occlusion after FDS placement. However, these studies have very varied methodologies: silicon
103 flow models [4], animal models [4,5], computational fluid dynamics (CFD) models [6,7],
104 digital subtraction angiography (DSA)-based optical flow approach [8], or patient cohort
105 studies [9,10]. To the best of our knowledge there is no pre-treatment predictive score available
106 in the literature for complete occlusion of IAs treated by FDS.

107 The purpose of our study was to propose a predictive score of complete occlusion of
108 IAs treated with FDS based on initial (i.e.: pre-treatment) clinical and angiographic criteria
109 (DIANES [diameter, indication, artery, neck, exit, sex] score) using machine learning.

110

111 **Methods**

112 *Patients*

113 The data that support the findings of this study are available from the corresponding
114 author upon reasonable request. We retrospectively reviewed in a prospectively maintained
115 database the data of patients consecutively treated in our Institution from October 2008 to
116 December 2019 by means of FDSs for IAs. Approval of the institutional review board was
117 obtained; without patient informed consent required. Exclusion criteria were: not assessable IA
118 (carotid-cavernous sinus fistula, parent artery occlusion), unavailable DSA images, and follow-
119 up < 6 months (loss to follow-up, death).

120 We systematically reviewed: patients' demographics: age, sex; IAs' characteristics:
121 type, location, configuration (saccular unilobular or complex [10] [fusiform, dysmorphic,
122 multilobular]), sizing, neck ratio (NR) [11] (ratio of diameters of the neck and the parent artery),
123 ruptured or unruptured IA, indication (first treatment, recanalization), presence of a side-branch
124 artery incorporated into the IA, and contrast agent stagnation at venous phase; parent artery'
125 characteristics: diameters (5 mm upstream to the neck and 5 mm downstream), diameters ratio
126 (PDR), curvature of the parent artery in relation to the tangent passing through the neck of the
127 IA (acute angle: concavity, no angle: straightness, obtuse angle: convexity), and inflow angle
128 [12]; as well as devices' characteristics: type, number, and associate coiling.

129

130 *Management*

131 Prior to the procedure, the neuroradiology team collegially assessed the characteristics
132 of each aneurysm and treatment modalities were discussed at a multidisciplinary meeting
133 (including neurosurgeons and neurointensivists).

134 All patients received dual-antiplatelet therapy (clopidogrel and aspirin) 5 days before
135 stenting. In case of clopidogrel resistance (assessed by a platelet-aggregation test: Multi-plate
136 [Roche Diagnostics]), patients were treated with ticagrelor for 6 months after the procedure. If

137 the platelet-aggregation test was satisfactory, patients were maintained on dual antiplatelet
138 therapy for at least 6 months after the procedure, followed by aspirin alone during 6 months.

139 Procedures were performed under general anesthesia through femoral access. The
140 FDSs were deployed using a tri-axial guiding-catheter system (using a 6 French long sheath, a
141 5 or 6F supple intermediate support catheter and a 0.027" microcatheter). Five commercially
142 available devices were used: the Pipeline Embolization Device (PED, PED Flex [Covidien]),
143 the Silk (Balt), the Flow-Redirection Endoluminal Device (FRED [MicroVention]), the Surpass
144 (Streamline, Evolve [Stryker]) and the p64 (Phenox).

145

146 *Outcome*

147 MRI was performed at 6-month, DSA at 1-year, and MRI/DSA at last follow-up. The
148 last follow-up is defined as the date with the last available imaging control of the aneurysmal
149 occlusion (by MRI or DSA). Based on their last follow-up, IAs were dichotomized as occluded
150 (RROC=A) or residual (RROC=B/C) [2]. A junior (in-training) and two senior interventional
151 neuroradiologists (with five and twelve years of experience) independently reviewed the
152 follow-up imaging studies, blinded to the clinical data. Discrepancies were settled by consensus
153 agreements. The primary outcome was the last available scoring for patients followed at least
154 6 months, with only RROC=A scored patients being considered successes.

155

156 *Statistical analysis*

157 80% of the aneurysm cases were randomly attributed to the learning set while the
158 remaining 20% were kept as an untouched test set. Subsequently, a separate set of 27 newly
159 gathered aneurysms was fused to the randomly selected test set. Quantitative variables were
160 discretized by manually selecting limits maximizing success/failure separation on the training
161 set close to the ones a rpart tree algorithm would have chosen using the "outcome" as variable
162 to be classified, yielding at least 20 cases per interval (subgroups being the result of splitting a
163 variable on the train set, and not each of the intersections of said split variable with the
164 "outcome" variable) and if possible, thresholds being rounded enough to make for a clinically

165 acceptable score. The impurity allowing class separation by an rpart tree was based on the
166 information index [13]. Feature selection and binary outcome prediction relied on elasticnet
167 [14] penalized logistic regression (LR). Class weighting accounted for the unequal number of
168 cases in the success and failure groups.

169 To enhance the interpretability and performance of the model, a subset of available
170 features may prove more efficient than the full feature range. We chose a genetic algorithm as
171 a means to explore the possible predictor variable combinations more efficiently than stepwise-
172 forward and -backward algorithms commonly used in medicine [15–17]. We ran the variable
173 selection genetic algorithm with a 0/1 numerical encoding (allowing for example a single
174 coefficient for gender=male to represent the gender variable, instead of having 2 opposite
175 coefficients). This well-described algorithm initially draws a number of predictor combinations,
176 and tests the predictive ability of logistic regressions using said combinations of predictors by
177 10-fold cross validation within the “train” cohort. Only the most efficient combinations are
178 allowed to proceed to the following generation, where a mixture of “mutation” (random
179 addition or deletion of a predictor within a combination) and “crossover” (the random matching
180 of the x-first variables a priori successful combination to the y-last of another combination)
181 creates new combinations to be tested.

182 The algorithm was allowed to proceed for 200 generations of 40 'genotypes' each (mutation
183 rate: 0.15, maximum features per genotype: 20). The penalization parameter 's' for predictions
184 was set to 0.02, and among the tested performance criteria (mean misclassification error, sum
185 or product of true positive rate and accuracy), prediction area under the curve proved the most
186 efficient (averaged prediction on the validation sample of each cross-validation performed on
187 the training dataset).

188 To obtain an efficient elasticnet mixing parameter, a grid tuning was subsequently
189 performed for each of the most promising feature sets from the precedent step with a second
190 cross validated penalized and weighted LR, always on the training subset of data. Each of the
191 selected feature sets with its proposed elasticnet mixing parameter was then used in a LR
192 trained on the full training dataset and evaluated by its max (accuracy + true positive rate)

193 over the range of thresholds (where FDS failure is considered as the positive class). The
194 model was transformed into score by extracting beta coefficients, and the threshold chosen to
195 maximize “accuracy + balanced accuracy” on the training set.

196 The interobserver reliability was assessed by calculation of Kappa (κ) values,
197 categorized as: 0.41-0.6, 0.61-0.8, and 0.81-1 indicating moderate, good, and excellent
198 agreement, respectively.

199 All statistical analyses were performed using R (3.4.1) and RStudio (1.0.153); packages
200 were: *car*, *caret*, *Hmisc*, *rpart*, *ggplot2*, *questionr*, *corrplot*, *dummies*, *pROC* and *reshape*.
201 Regression was done using *glmnet* embedded in the *mlr* package.

202

203

204 **Results**

205 *Clinical Characteristics*

206 One hundred and seventy-nine patients were screened for eligibility during the study
207 period. Thirty-three patients were excluded for lost to follow-up (n=25), parent artery occlusion
208 (n=3), death (n=4), and FDS for carotid-cavernous fistula treatment (n=1). The four early (<6
209 months) deaths were due to: an early hematoma with death at the eighth day after the treatment
210 with FDS and coils of a giant aneurysm of the middle cerebral artery, a complication of dual
211 anti-platelet therapy with death twenty-three days after stenting, a retroperitoneal hematoma
212 requiring the interruption of dual anti-platelet therapy leading to cerebral ischemic and
213 hemorrhagic complication with death on the seventh day, and a fatal hemorrhagic
214 transformation after cerebral infarction. The parent artery occlusions by coils were due to one
215 intra-aneurysmal stent migration in a giant intracavernous aneurysm and two misopening of the
216 FDS. One hundred forty-six patients (one hundred fifty-four IAs) were included in this study.
217 They were randomly assigned to the learning cohort (80%) or the validation cohort (20%).
218 Patients, IAs and parent arteries pre-stenting characteristics are summarized in **Table 1**. The
219 overall median follow-up was 14.4 months (interquartile range [IQR]: 11.9–30.4). The
220 distribution of the devices was as follows: nitinol: n = 18 Silk (11%), n = 2 FRED (1.2%), n =
221 4 p64 (2.4%) and cobalt-chromium alloy: n = 128 PED (78%), n = 12 Surpass (7.3%). A second
222 telescopic FDS was required in ten cases (6.5%). No procedure required more than two FDS.
223 In 23 cases (14.9%), the coiling of the aneurysmal sac was performed before stenting because
224 of the large diameter of the IA (median diameter: 10 mm, IQR: 6.9–13.9). 117 IAs were
225 assigned to group RROC=A (complete obliteration), 37 IAs were assigned to group
226 RROC=B/C (n=15 for residual neck and n=22 for residual IA, respectively). Interreader
227 agreement for RROC status evaluated at last follow-up by MRI or DSA was considered as
228 excellent with $\kappa = 0.88$ (95%CI: 0.79–0.98) and good for the assessment of side-branch artery
229 and parent artery curvature: $\kappa = 0.78$ (95%CI: 0.62–0.96) and $\kappa = 0.71$ (95%CI: 0.53–0.90),
230 respectively. The median of the last follow-up was 14.9 months (IQR: 12.1–29.8) and the mean
231 was 23.3 months (standard deviation [SD]=18.2 months) in the RROC=A group, and the

232 median of the last follow-up was 13.4 months (IQR: 10.1–30.8) and the mean was 22.0 months

233 (SD=19.5 months) in the RROC=B/C group.

234

235 **Table 1: Patients, Intracranial Aneurysms and Parent Arteries Initial Characteristics**

Parameters	Train	Test
Patients	98	51
Female	77 (79)	44 (86)
Age (years)*	50 (39–56)	54 (45–59)
Intracranial aneurysms (IAs)	102	52
Diameter (mm) *	7 (5–9.88)	6.31 (4.25–12.48)
Neck (mm)*	4.6 (3.5–6.15)	4.82 (3.92–6.73)
Dome-to-neck ratio (DNR)*	1.4 (1.08–1.79)	1.39 (1.14–2)
Locations:		
Anterior circulation: Carotid-ophthalmic	40	24
Posterior communicating artery	12	4
Supraclinoid ICA	4	0
Cavernous ICA	10	3
ICA Siphon	5	11
Anterior communicating and anterior cerebral arteries	5	3
Middle cerebral artery	5	1
Anterior choroidal artery	1	3
Superior hypophyseal artery	1	2
Posterior circulation: Vertebral artery	8	0
Posterior cerebral artery	4	0
Basilar artery	4	0
Superior and posterior inferior cerebellar arteries	3	1
Type:		
Saccular	82 (80.4)	45 (86.5)
Dissecting aneurysm	4 (3.9)	1 (1.9)
Large/giant partially thrombosed	8 (7.8)	1 (1.9)
Fusiform	4 (3.9)	0
Blister-like	4 (3.9)	5 (9.6)
Indication: Recanalization	34 (33)	14 (27)
Ruptured IA	27 (26)	12 (23)
Contrast media stagnation	27 (26)	18 (35)
Incorporated side-branch artery: Yes	18 (18)	12 (23)
Diameter (mm)*	1.1 (0.8–1.5)	1.15 (0.97–1.53)
Configuration: Complex	82 (80)	45 (87)
Parent arteries		
Diameters: Upstream (mm)*	3.7 (3.1–4.1)	4.1 (3.57–4.5)
Downstream (mm)*	3.1 (2.62–3.4)	3.2 (2.87–3.6)
Average (mm) *	3.35 (2.91–3.74)	3.65 (3.28–4.03)
Upstream/downstream ratio (PDR) *	1.19 (1.06–1.37)	1.26 (1.14–1.36)
Neck / parent artery diameters ratio (NR)*	1.44 (1.03–1.95)	1.34 (1.07–1.87)

Geometry: Inflow angle (degree °)*	135 (95–163)	135 (103–168)
Convex Curvature	50 (49)	20 (38)

236

237 Note: unless otherwise indicated, data are number of patients, with percentage in brackets.

238 * Data are median with the interquartile range (IQR) in brackets.

239 ICA = internal carotid artery, n = number, NR = neck ratio, PDR = parent artery diameters ratio.

240

241 *Training Sample*

242 Six variables were included in the DIANES score. The score ranged from -24 to 4
 243 points (**Table 2**). The median score was -3 (IQR: -7–2) in the overall cohort. Among failed
 244 occlusion (RROC=B/C) the median score was -8 (IQR: -10–5) and -2 (IQR: -4–2) among
 245 successful occlusion (RROC=A). In receiver operating characteristic analysis, a score greater
 246 than -6 maximized the ability to predict a complete occlusion (RROC=A). The score accuracy
 247 was 0.86 (95% CI: 0.79–0.94), with sensitivity of 0.87 (95% CI: 0.79–0.95) and specificity of 0.82
 248 (95% CI: 0.64–0.96) (**Table 3, Fig 1**).

249

250 *Test Sample and Whole Cohort*

251 In the test sample, a DIANES score greater than -6 was predictive of complete
 252 occlusion (RROC=A), with sensitivity of 0.89 (95% CI: 0.77–0.98) and specificity of 0.60 (95% CI:
 253 0.33–0.86). The score accuracy was 0.81 (95% CI: 0.69–0.91) (**Table 3, Fig 1**). In the whole
 254 cohort, a DIANES score greater than -6 was predictive of complete occlusion (RROC=A), with
 255 sensitivity of 0.88 (95% CI: 0.82–0.94) and specificity of 0.73 (95% CI: 0.58–0.87). The score
 256 accuracy was 0.84 (95% CI: 0.78–0.90) (**Table 3, Fig 1**). The DIANES score was able to divide
 257 the whole cohort from either side of the threshold value (-6 points) in both success (RROC=A)
 258 and failure (RROC=B/C) groups at last follow-up (**Fig 1**). Additional representations have been
 259 added to the supplemental material with their accuracies (95% CI) on training and test samples: a
 260 recursive partitioning CART tree, a penalized logistic regression LASSO, and a simplified
 261 version of the DIANES score.

262 **Table 2:** DIANES Score Components and Scoring Parameters
 263

Component	Score
1. Sex	
Male	4
2. Indication	
Recanalization	-5
3. Side-branch artery	
Yes	-8
4. Aneurysm's diameter (mm)	
> 8.9	-5
5. Neck ratio (NR)	
> 1.1 ; 1.8 ≤	-2
6. Parent artery diameters ratio (PDR)	
> 1.3	-4
Threshold (under = predictive of failure)	-6

264

265 Note: the score is the sum of the points of the seven criteria. The threshold maximizing class
 266 separation (i.e.: RROC=A and RROC=B/C), a score below two was predictive of incomplete
 267 occlusion (RROC=B/C).

268 DIANES score = diameter, indication, artery, neck, exit, sex score, RROC = Raymond-Roy
 269 occlusion classification.

270
 271
 272
 273

Table 3: Sensitivities, Specificities and Predictive Values for the DIANES Score

	Accuracy	Sensitivity	Specificity	Positive Predictive Value (PPV)	Negative Predictive Value (NPV)	AUC
Training sample	0.86 (0.79, 0.94)	0.87 (0.79, 0.95) [70 / 80]	0.82 (0.64, 0.96) [18 / 22]	0.95 (0.88, 0.99) [70 / 74]	0.64 (0.45, 0.83) [18 / 28]	0.88 (0.80, 0.96)
Test sample	0.81 (0.69, 0.91)	0.89 (0.77, 0.98) [33 / 37]	0.60 (0.33, 0.86) [9 / 15]	0.86 (0.72, 0.95) [33 / 37]	0.66 (0.41, 0.93) [9 / 13]	0.73 (0.55, 0.91)
Whole cohort	0.84 (0.78, 0.90)	0.88 (0.82, 0.94) [103 / 117]	0.73 (0.58, 0.87) [27 / 37]	0.91 (0.85, 0.96) [103 / 113]	0.66 (0.51, 0.81) [27 / 41]	0.83 (0.74, 0.91)

274

275 Note: Data are percentages; data in parentheses are 95% confidence intervals (CIs); data in
 276 brackets are numerator/denominator.

277 DIANES score = diameter, indication, artery, neck, exit, sex score.

278 **Discussion**

279 The evolution of the clinical practice and the current knowledge in the field of FDS
280 requires a better prediction of IA occlusion after stenting by FDS. Currently, the prediction of
281 IA's thrombosis can either be based on descriptive grading scales using DSA images [18,19],
282 parametric color coding [20] or CFD models [21]. Furthermore, off-label applications of the
283 FDSs have been reported [22] such as ruptured IAs [23], requiring an even more accurate
284 prediction. Moreover, FDSs are associated with an elevated rate (34%) of ipsilateral de novo
285 fluid-attenuated inversion recovery (FLAIR) lesions, most likely due to delayed
286 thromboembolic events from the FDS/IA complex before complete healing of the IA [24].

287 In our cohort, the DIANES score is associated with long-term aneurysmal sac occlusion
288 in patients treated with FDS. The score is based on six items: two clinical criteria (**i**/sex,
289 **ii**/indication) and four imaging criteria regarding the morphology of the IA (**iii**/side-branch
290 artery, **iv**/diameter, **v**/NR) and the parent artery (**vi**/PDR). These criteria have already been
291 described as predictive in the literature.

292 Regarding the clinical criteria of the score: **i**/The DIANES score reflects vascular gender
293 differences, with males predicting a higher occlusion rate. Indeed, sex steroid hormones are
294 well-known factors involved in IAs' pathogenesis [25] but their role in vascular remodeling
295 after stenting is poorly known. Moreover, circulating bone marrow-derived endothelial
296 progenitor cells (PCs) play an important role in vascular repair [26] and endothelialization of
297 the FDS's mesh [26]. However, women have lower PCs levels compared to men and are likely
298 to reach a critically low level with aging [27] ; **ii**/In our score, an FDS indication for a
299 recanalized IA is a less favorable situation. Healing of a coiled IA is a dynamic process
300 occurring within the first four weeks after embolization and recanalization occurs in 10-20% of
301 cases [28]. Indeed, although FDSs are a well-recognized treatment of recurrent IAs, it could be
302 hypothesized that several mechanisms underlying the recanalization pathophysiology [28] such
303 as active vascular wall disease, poor quality neointima formation across the neck, or significant
304 transmission of blood pulsation affecting the thrombus stability [5] may also affect the efficacy
305 of the stent.

306 Regarding the morphological criteria of the score: **iii**/The existence of a side-branch artery
307 arising from the sac has been previously demonstrated as a negative predicting factor for IA's
308 occlusion [9,29] diminishing the 'flow-diverting effect'; **iv**/FDS seems to be a relatively safe
309 and effective technique for large and giant unruptured IAs embolization [30] but the success of
310 occlusion could depend on the neck size [4]. In these cases, occlusion failures could be
311 explained by holes in the neointima lining the FDS [31] ; **v**/In the literature, NR was described
312 as a predictive factor of occlusion [11], whereas larger neck diameters [4,5] and lower dome-
313 to-neck ratios [29] were negative predictive criteria. The NR is a predictor of failure and
314 suggests that a larger defect in the parent artery provides the input for blood flow into RROC
315 B/C IAs. This would result in higher flow in the IA sac, which represents a greater burden for
316 flow diversion and thus less effective treatment of FDS [11]. Ostium enlargement has been
317 correlated with the rate of IA occlusion after flow diversion in animal model studies [4,32];
318 **vi**/At last, in our score, a higher PDR could also reflect an increased risk of FDS oversizing and
319 poor wall apposition. Oversizing could be associated with lower pore density and metal
320 coverage resulting in increased porosity of the FDS [33] and malapposition [29] results in the
321 risk of endoleak and failure of endothelialization.

322 During the follow-up period of IAs treated with FDSs, there was no further treatment
323 of the IAs. The reasons for the lack of a second treatment was that the majority of IAs were
324 unruptured, occlusion of the IA could occur in the medium to long term, and in most cases the
325 only additional treatment available would be another FDS which would increase the risks
326 associated with this device.

327 The statistical model chosen was a genetic algorithm for the selection of variables.
328 Genetic algorithms do not guarantee to obtain the global maximum accuracy but represent a
329 trade-off between greedy algorithms like stepwise ascent or descent, and extreme time-
330 consuming exploration of all available predictor variable combinations. Mimicking aspects of
331 Darwinian processes for machine learning was already hypothesized as a fruitful branch to
332 explore by Alan Turing in 1950, and progressively came to use in the 1970s and 1980s. Genetic
333 algorithms usually outperform stepwise ascent or descent in variable selection for model

334 creation [15,16]. Recently, machine learning analysis has been used in the field of
335 interventional neuroradiology [34,35].

336 We acknowledge potential limitations of our study, including the need for an external
337 validation of the score with patients from different centers and larger cohorts. We recognize the
338 relative complexity of the score given the variance of the weighting, but it includes only six
339 variables that can be easily and routinely assessed from the clinic and imaging data. In addition,
340 the possibility of very late appearance of complete thrombosis in an initially RROC=B/C IA
341 cannot be ruled out. Also, we have chosen to include ten patients treated with two FDSs as this
342 variable was not retained during the statistical selection step and furthermore, this factor is not
343 usually used in predictive studies. Finally, the IA thrombosis is a complex spatio-temporal
344 process mediated by several mechanisms such as vascular morphology, biochemical factors
345 produced by the IA wall, blood flow patterns and biomechanical factors of the FDS including
346 endothelialization of the device's struts, and should thus not be limited to clinico-angiographic
347 data. Our score was developed for its ability to predict the occlusion of an IA treated with FDS;
348 it does not take into account other important outcomes in the choice of treatment such as the
349 occurrence of a complication (e.g. ischemic stroke).

350 This opens the field of a more personalized patient management because of an IA-specific
351 complete thrombosis threshold [21]. Despite these limitations, improved standardization of pre-
352 treatment assessment with the use of the DIANES score is intended to provide a radioclinical
353 tool to predict success after FDS implantation in routine clinical care. This score may provide
354 a predictive stratification of FDS success for assessment of new treatments in therapeutic trials.

355

356

357

358

359

360

361

362 **Conclusions**

363 The DIANES score presented herein, which includes pre-treatment clinical factors and
364 imaging morphological features of both the IA and the parent artery, showed an association
365 with the final occlusion status. This clinico-radiological grading scale, built on components
366 easily assessed routinely, needs to be tested in a larger separate validation cohort and could be
367 used for the selection of therapeutic alternatives for exclusion treatment in patients with IAs.

368

369

370

371

372

373

374

375

376

377

378

379

380

381

382

383

384

385

386

387

388

389

390

391

392 **Disclosures**

393 Pr Frédéric Clarençon reports conflict of interest with Medtronic, Guerbet, Balt Extrusion
394 (payment for readings), Codman Neurovascular (core lab). Dr Nader Sourour is consultant for
395 Medtronic, Balt Extrusion, Microvention, Stock/Stock Options: Medina. The other authors
396 report no conflict of interest concerning the materials or methods used in this study or the
397 findings specified in this paper. The manuscript is not supported by industry.

398

399 **Competing Interests**

400 None.

401

402 **Contributorship Statement**

403 Conception and design: AG, CT, FC; Acquisition of data: AG, ES, NS, FC; Analysis and
404 interpretation of data: AG, CT, FC; Drafting the article: AG, CT, FC; Critically revising the
405 article: ES, JG, BM, KP, SL, VD; Reviewed submitted version of manuscript: AG, CT, FC;
406 Approved the final version of the manuscript on behalf of all authors: FC.

407 **Funding**

408 None.

409

410 **Data Availability**

411 The data that support the findings of this study are available from the corresponding author
412 upon reasonable request.

413

414 **Research Ethics Approval**

415 Approval of the institutional review board was obtained (CPP-Ile-de-France VI, Groupe
416 Hospitalier Pitié-Salpêtrière, Pr Nathalie BRION, June 14th 2019); without patient informed
417 consent required.

418

419

420

421

References

422

1 Brinjikji W, Murad MH, Lanzino G, *et al.* Endovascular Treatment of Intracranial Aneurysms With Flow Diverters: A Meta-Analysis. *Stroke* 2013;**44**:442–7.

423

doi:10.1161/STROKEAHA.112.678151

424

425

2 Roy D, Milot G, Raymond J. Endovascular treatment of unruptured aneurysms. *Stroke*

426

2001;**32**:1998–2004. doi:10.1161/hs0901.095600

427

3 Becske T, Kallmes DF, Saatci I, *et al.* Pipeline for Uncoilable or Failed Aneurysms:

428

Results from a Multicenter Clinical Trial. *Radiology* 2013;**267**:858–68.

429

doi:10.1148/radiol.13120099

430

4 Gentric JC, Darsaut TE, Makoyeva A, *et al.* The Success of Flow Diversion in Large and Giant Sidewall Aneurysms May Depend on the Size of the Defect in the Parent Artery.

431

Am J Neuroradiol 2014;**35**:2119–24. doi:10.3174/ajnr.A4010

432

433

5 Cebral JR, Mut F, Raschi M, *et al.* Analysis of Hemodynamics and Aneurysm Occlusion after Flow-Diverting Treatment in Rabbit Models. *Am J Neuroradiol* 2014;**35**:1567–73.

434

doi:10.3174/ajnr.A3913

435

436

6 Xiang J, Damiano RJ, Lin N, *et al.* High-fidelity virtual stenting: modeling of flow diverter deployment for hemodynamic characterization of complex intracranial

437

aneurysms. *J Neurosurg* 2015;**123**:832–40. doi:10.3171/2014.11.JNS14497

438

439

7 Mut F, Raschi M, Scrivano E, *et al.* Association between hemodynamic conditions and occlusion times after flow diversion in cerebral aneurysms. *J NeuroInterventional Surg*

440

2015;**7**:286–90. doi:10.1136/neurintsurg-2013-011080

441

442

8 Pereira VM, Bonnefous O, Ouared R, *et al.* A DSA-Based Method Using Contrast-Motion Estimation for the Assessment of the Intra-Aneurysmal Flow Changes Induced

443

by Flow-Diverter Stents. *Am J Neuroradiol* 2013;**34**:808–15. doi:10.3174/ajnr.A3322

444

445

9 Brasiliense LBC, Aguilar-Salinas P, Miller DA, *et al.* Analysis of Predictors and Probability of Aneurysm Occlusion in the Internal Carotid Artery After Treatment with Pipeline Embolization Device. *World Neurosurg* 2017;**107**:641–8.

446

doi:10.1016/j.wneu.2017.08.099

447

448

449

10 Dodier P, Frischer JM, Wang W-T, *et al.* Immediate Flow Disruption as a Prognostic Factor After Flow Diverter Treatment: Long-Term Experience with the Pipeline

450

Embolization Device. *World Neurosurg* 2018;**113**:e568–78.

451

doi:10.1016/j.wneu.2018.02.096

452

453

11 Paliwal N, Tutino VM, Shallwani H, *et al.* Ostium Ratio and Neck Ratio Could Predict the Outcome of Sidewall Intracranial Aneurysms Treated with Flow Diverters. *Am J*

454

Neuroradiol 2019;**40**:288–94. doi:10.3174/ajnr.A5953

455

456

12 Beller E, Klopp D, Göttler J, *et al.* Closed-Cell Stent-Assisted Coiling of Intracranial Aneurysms: Evaluation of Changes in Vascular Geometry Using Digital Subtraction

457

Angiography. *PLOS ONE* 2016;**11**:e0153403. doi:10.1371/journal.pone.0153403

458

459

13 Therneau TM, Atkinson EJ. An Introduction to Recursive Partitioning Using the RPART Routines. Mayo Foundation. Cranr-Proj. 2019.[https://cran.r-](https://cran.r-project.org/web/packages/rpart/vignettes/longintro.pdf)

460

[project.org/web/packages/rpart/vignettes/longintro.pdf](https://cran.r-project.org/web/packages/rpart/vignettes/longintro.pdf) (accessed 26 Oct 2020).

461

- 462 14 Zou H, Hastie T. Regularization and Variable Selection via the Elastic Net. *J R Stat Soc*
463 *Ser B Stat Methodol* 2005;**67**:301–20.
- 464 15 Vinterbo S, Ohno-Machado L. A genetic algorithm to select variables in logistic
465 regression: example in the domain of myocardial infarction. *Proc AMIA Symp*
466 1999;;984–8.
- 467 16 Johnson P, Vandewater L, Wilson W, *et al.* Genetic algorithm with logistic regression for
468 prediction of progression to Alzheimer’s disease. *BMC Bioinformatics* 2014;**15**:S11.
469 doi:10.1186/1471-2105-15-S16-S11
- 470 17 Sale M, Sherer EA. A genetic algorithm based global search strategy for population
471 pharmacokinetic/pharmacodynamic model selection: Genetic algorithm in PK/PD model
472 selection. *Br J Clin Pharmacol* 2015;**79**:28–39. doi:10.1111/bcp.12179
- 473 18 Kamran M, Yarnold J, Grunwald IQ, *et al.* Assessment of angiographic outcomes after
474 flow diversion treatment of intracranial aneurysms: a new grading schema.
475 *Neuroradiology* 2011;**53**:501–8. doi:10.1007/s00234-010-0767-5
- 476 19 Grunwald IQ, Kamran M, Corkill RA, *et al.* Simple Measurement of Aneurysm Residual
477 after Treatment: the SMART scale for evaluation of intracranial aneurysms treated with
478 flow diverters. *Acta Neurochir (Wien)* 2012;**154**:21–6. doi:10.1007/s00701-011-1177-0
- 479 20 Göllitz P, Struffert T, Rösch J, *et al.* Cerebral aneurysm treatment using flow-diverting
480 stents: in-vivo visualization of flow alterations by parametric colour coding to predict
481 aneurysmal occlusion: preliminary results. *Eur Radiol* 2015;**25**:428–35.
482 doi:10.1007/s00330-014-3411-7
- 483 21 Kulcsár Z, Augsburger L, Reymond P, *et al.* Flow diversion treatment: intra-aneurysmal
484 blood flow velocity and WSS reduction are parameters to predict aneurysm thrombosis.
485 *Acta Neurochir (Wien)* 2012;**154**:1827–34. doi:10.1007/s00701-012-1482-2
- 486 22 Murthy SB, Shah J, Mangat HS, *et al.* Treatment of Intracranial Aneurysms With
487 Pipeline Embolization Device: Newer Applications and Technical Advances. *Curr Treat*
488 *Options Neurol* 2016;**18**:16. doi:10.1007/s11940-016-0399-0
- 489 23 Lin N, Brouillard AM, Keigher KM, *et al.* Utilization of Pipeline embolization device for
490 treatment of ruptured intracranial aneurysms: US multicenter experience. *J*
491 *NeuroInterventional Surg* 2015;**7**:808–15. doi:10.1136/neurintsurg-2014-011320
- 492 24 Safain MG, Roguski M, Heller RS, *et al.* Flow Diverter Therapy With the Pipeline
493 Embolization Device Is Associated With an Elevated Rate of Delayed Fluid-Attenuated
494 Inversion Recovery Lesions. *Stroke* 2016;**47**:789–97.
495 doi:10.1161/STROKEAHA.115.010522
- 496 25 Boese AC, Kim SC, Yin K-J, *et al.* Sex differences in vascular physiology and
497 pathophysiology: estrogen and androgen signaling in health and disease. *Am J Physiol-*
498 *Heart Circ Physiol* 2017;**313**:H524–45. doi:10.1152/ajpheart.00217.2016
- 499 26 Iwakura A, Luedemann C, Shastry S, *et al.* Estrogen-Mediated, Endothelial Nitric Oxide
500 Synthase-Dependent Mobilization of Bone Marrow-Derived Endothelial Progenitor
501 Cells Contributes to Reendothelialization After Arterial Injury. *Circulation*
502 2003;**108**:3115–21. doi:10.1161/01.CIR.0000106906.56972.83

- 503 27 Topel ML, Hayek SS, Ko Y, *et al.* Sex Differences in Circulating Progenitor Cells. *J Am*
504 *Heart Assoc* 2017;**6**. doi:10.1161/JAHA.117.006245
- 505 28 Brinjikji W, Kallmes DF, Kadirvel R. Mechanisms of Healing in Coiled Intracranial
506 Aneurysms: A Review of the Literature. *Am J Neuroradiol* 2015;**36**:1216–22.
507 doi:10.3174/ajnr.A4175
- 508 29 Shapiro M, Becske T, Nelson PK. Learning from failure: persistence of aneurysms
509 following pipeline embolization. *J Neurosurg* 2017;**126**:578–85.
510 doi:10.3171/2015.12.JNS152065
- 511 30 Cagnazzo F, Mantilla D, Rouchaud A, *et al.* Endovascular Treatment of Very Large and
512 Giant Intracranial Aneurysms: Comparison between Reconstructive and Deconstructive
513 Techniques—A Meta-Analysis. *Am J Neuroradiol* 2018;**39**:852–8.
514 doi:10.3174/ajnr.A5591
- 515 31 Darsaut TE, Bing F, Makoyeva A, *et al.* Flow Diversion of Giant Curved Sidewall and
516 Bifurcation Experimental Aneurysms with Very-Low-Porosity Devices. *World*
517 *Neurosurg* 2014;**82**:1120–6. doi:10.1016/j.wneu.2013.09.036
- 518 32 Chung B, Mut F, Kadirvel R, *et al.* Hemodynamic analysis of fast and slow aneurysm
519 occlusions by flow diversion in rabbits. *J NeuroInterventional Surg* 2015;**7**:931–5.
520 doi:10.1136/neurintsurg-2014-011412
- 521 33 Makoyeva A, Bing F, Darsaut TE, *et al.* The Varying Porosity of Braided Self-Expanding
522 Stents and Flow Diverters: An Experimental Study. *Am J Neuroradiol* 2013;**34**:596–602.
523 doi:10.3174/ajnr.A3234
- 524 34 Podgorsak AR, Rava RA, Shiraz Bhurwani MM, *et al.* Automatic radiomic feature
525 extraction using deep learning for angiographic parametric imaging of intracranial
526 aneurysms. *J NeuroInterventional Surg* 2020;**12**:417–21. doi:10.1136/neurintsurg-2019-
527 015214
- 528 35 Ramos LA, van der Steen WE, Sales Barros R, *et al.* Machine learning improves
529 prediction of delayed cerebral ischemia in patients with subarachnoid hemorrhage. *J*
530 *NeuroInterventional Surg* 2019;**11**:497–502. doi:10.1136/neurintsurg-2018-014258
- 531
532
533

534 **Figure 1 Legends:**

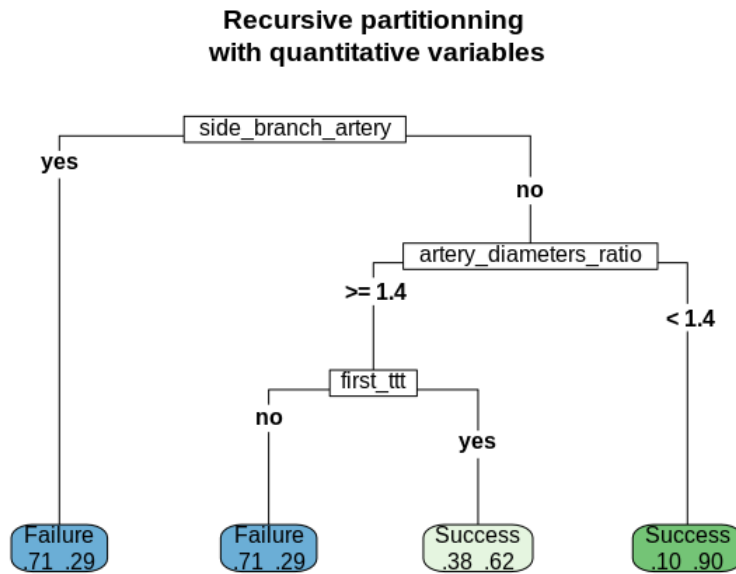
535 **Above:** Graphs showing receiver operating characteristic (ROC) curves with area under the
536 curve (AUC) and 95% confidence intervals (CIs) for occlusion prediction in the training sample
537 (A), in the test sample (B), and in the whole cohort (C).

538 **Below:** Dot plot displaying patients' distribution from either side of the threshold value of the
539 DIANES score (two points) in both success (RROC=A) and failure (RROC=B/C) groups at last
540 follow-up in the whole cohort.

541 DIANES score = diameter, indication, artery, neck, exit, sex score, RROC = Raymond-Roy
542 occlusion classification.

Supplemental material:

Recursive partitioning CART tree from the quantitative variables:



CART tree	Accuracy	Sensitivity	Specificity	Positive Predictive Value (PPV)	Negative Predictive Value (NPV)	Balanced Accuracy
Training sample	0.8137 95% CI : (0.7245, 0.884)	0.8500	0.6818	0.9067	0.5556	0.7659
Test sample	0.7692 95% CI : (0.6316, 0.8747)	0.8649	0.5333	0.8205	0.6154	0.6991

Penalized logistic regression LASSO from qualitatively rendered variables:

Component	Score
Sex: Male	0.8
Indication: Recanalization	-1
Side-branch artery: Yes	-1.1
Aneurysm's diameter (mm): > 8.9	-1.1
Parent artery diameters ratio (PDR): > 1.3	-0.8
Neck ratio (NR): > 1.1 ; 1.8 ≤	-0.4
Neck ratio (NR): > 1.8	0.2
Convexity of the parent artery	-0.2
Threshold (under = predictive of failure)	0.75

LASSO	Accuracy	Sensitivity	Specificity	Positive Predictive Value (PPV)	Negative Predictive Value (NPV)	Balanced Accuracy
Training sample	0.8725 95% CI : (0.7919, 0.9304)	0.8875	0.8182	0.9467	0.6667	0.8528
Test sample	0.7885 95% CI : (0.653, 0.8894)	0.9189	0.4667	0.8095	0.7000	0.6928

Simplified version of the DIANES score:

Component	Score
1. Sex	
Male	2
Female	-2
2. Indication	
First treatment	2
Recanalization	-2
3. Side-branch artery	
No	3
Yes	-3
4. Aneurysm's diameter (mm)	
≤ 8.9	2
> 8.9	-2
5. Neck ratio (NR)	
≤ 1.1	1
> 1.1 ; 1.8 ≤	-1
> 1.8	1
6. Parent artery diameters ratio (PDR)	
≤ 1.3	2
> 1.3	-2
Threshold (under = predictive of failure)	-1

Simplified DIANES score	Accuracy	Sensitivity	Specificity	Positive Predictive Value (PPV)	Negative Predictive Value (NPV)	AUC
Training sample	0.87 (0.80 - 0.94)	0.91 (0.84 - 0.96) [73 / 80]	0.72 (0.52 - 0.91) [16 / 22]	0.92 (0.86 - 0.98) [73 / 79]	0.69 (0.5 - 0.88) [16 / 23]	0.88 (0.80 - 0.97)
Test sample	0.77 (0.65 - 0.89)	0.92 (0.82 - 1) [34 / 37]	0.40 (0.59 - 0.66) [6 / 15]	0.79 (0.66 - 0.91) [34 / 43]	0.67 (0.33 - 1) [6 / 9]	0.70 (0.52 - 0.89)
Whole cohort	0.84 (0.77 - 0.90)	0.91 (0.86 - 0.67) [107 / 117]	0.60 (0.41 - 0.75) [22 / 37]	0.88 (0.81 - 0.94) [107 / 122]	0.69 (0.52 - 0.85) [22 / 32]	0.82 (0.73 - 0.91)

